Polycyclic aromatic hydrocarbons (PAHs), oxy- and nitro-PAHs in ambient air of Arctic town Longyearbyen, Svalbard

Tatiana Drotikova[1,2*], Aasim M. Ali[2], Anne Karine Halse[3], Helena C. Reinardy[4,1], and Roland Kallenborn[2,1]

[1]University Centre in Svalbard (UNIS), Department of Arctic Technology, Longyearbyen, Svalbard, Norway
[2]Norwegian University of Life Sciences (NMBU), Faculty of Chemistry, Biotechnology and Food Sciences, Ås, Norway
[3]Norwegian Institute for Air Research (NILU), Department of Environmental Chemistry, Kjeller, Norway
[4]Scottish Marine Institute (SAMS), Department of Aquaculture and Environment, Oban, Argyll, PA37 1QA, UK

Correspondence to: Tatiana M. Drotikova (tatiana.drotikova@unis.no)

Abstract. Polycyclic aromatic hydrocarbons (PAHs) are not declining in Arctic air despite reductions in their global emissions. In Svalbard, the Longyearbyen coal-fired power plant is considered to be one of the major local source of PAHs. Power plant stack emissions and ambient air samples, collected simultaneously 1 km (UNIS) and 6 km (Adventdalen) transect distance, were analyzed (gaseous and particulate phases separately) for 22 nitro-PAHs, 9 oxy-PAHs and 16 parent PAHs by GC/ECNI/MS and GC-MS/MS. Results confirm low level of PAH emissions ($\sum$16 PAHs = 1.5 µg kg^{-1} coal) from the power plant. Phenathrene, 9,10-anthraquinone, 9-fluorenone, fluorene, fluoranthene, and pyrene accounted for 85% of the plant emission (not including naphthalene). A dilution effect was observed for the transect ambient air samples, 1.26 ± 0.16 and 0.63 ± 0.14 ng m^{-3} sum all 47 PAH derivatives for UNIS and Adventdalen, respectively. The PAH profile was homogeneous for these recipient stations with phenathrene and 9-fluorenone being most abundant. Principal component analysis, in combination with PAH diagnostic ratios and literature data on different source-specific markers, confirmed coal combustion, gasoline, and diesel traffic as the predominant sources of PAHs. Secondary atmospheric formation of 9-nitroanthracene and 2+3-nitrofluoranthene was evaluated and concluded. Results also indicate that ambient PAH concentrations were affected by precipitation events, and specific humidity is an essential parameter influencing PAH scavenging from the air. The present study contributes important data which can be utilized to eliminate uncertainties in model predictions that aim to assess the extent and impacts of Arctic atmospheric contaminants.

1 Introduction

Traditionally, Arctic regions are considered to be pristine and remote from the majority of potential large-scale emission sources in industrialized middle latitude countries (Armitage et al., 2011; Macdonal et al., 2000; Barrie et al., 1992). Atmospheric transport is the most efficient way for polycyclic aromatic hydrocarbons (PAHs), released in the lower latitudes, to reach the Arctic (Friedman et al., 2014). Long range atmospheric transport (LRAT) to Arctic regions has strong seasonality with an increased tendency during winter and spring (Willis et al., 2018)**.** This is driven by a different mean circulation direction across the Arctic in winter compared to summer, the extension and significantly increased permeability of the Arctic front in winter, and the absence of wet removal of particles during transport (Willis et al., 2018). These factors explain observed maximum near-surface pollutant concentrations during winter and minimum levels during summer (Klonecki, 2003). Fossil fuel sources dominate total aerosol organic carbon in Arctic winter air, with a predominance of alkanes, PAHs, and phthalates (Fu et al., 2009). During the past decades, the background monitoring of atmospheric pollutants in Ny-Ålesund, Svalbard, and Alert, Canada, have been an important data repository for information on occurrence and LRAT of anthropogenic contaminants including persistent organic pollutants and PAHs in the Arctic regions. The data demonstrates ubiquitous distribution of PAHs on a global scale, including the Arctic. "Confirmed occurrence of a pollutant in a polar environment" is an important criterion considered by conventions, including the United Nations Economic Commission for Europe (UNECE), Stockholm, Basel, and Rotterdam (Fiedler et al., 2019). UNECE has

incorporated PAHs in the Convention on Long-range Transboundary Air Pollution (UNECE, 1998). PAHs are regulated in many countries, eg. US, Canada, Holland, Sweden, Switzerland, and Denmark (Bandowe and Meusel, 2017). PAHs are also included in the list of target chemicals of the Convention for the Protection of the Marine Environment of the North-East Atlantic (OSPAR). PAH concentrations are not declining in the Arctic despite global emission reductions (Yu et al., 2019),

45 and PAHs are listed as "chemicals of emerging concern in the Arctic" (Balmer and Muir, 2017).

PAHs are byproducts of different incomplete combustion processes, mainly fossil fuels and biomass burning. Their toxic and carcinogenic effects on both human health and ecosystems are well documented (Kim et al., 2013; Reynaud and Deschaux, 2006; Macdonald et al., 2010). Under unique Arctic weather conditions, with extreme temperatures, wind, and light seasonality, atmospheric PAHs may behave differently compared to in temperate climatic conditions. Low temperatures

50 favor partitioning of semi-volatile PAHs from gas phase to particulate phase, which makes them more persistent in the Arctic environment (Lammel, 2015). Due to extended winter darkness in the Arctic, photodegradation of PAHs is limited for several months. The transition from dark polar winter to the light spring and summer brings large increase in the amount of available solar radiation and oxidants in the Arctic troposphere (Willis et al., 2018). PAHs react with a number of atmospheric oxidants, most notably the hydroxyl radical, ozone, the nitrate radical, and nitrogen dioxide (Keyte et al., 2013).

55 This leads to their transformation into more toxic oxygenated and nitrated PAH derivatives (oxy-PAHs and nitro-PAHs). Oxy- and nitro-PAHs are also constituents of raw coal and can be emitted with PAHs following the same combustion processes (Huang et al., 2014b). Oxy- and nitro-PAHs have high toxicity (Onduka et al., 2012); they can act as direct mutagens, carcinogens, and oxidative stressors in biota (Durant et al., 1996). The biological effects of nitro- and oxy-PAHs can be greater than those of the parent PAHs (Kielhorn et al., 2003). In remote locations they are found at concentrations

60 near detection limits and thus are mostly not included in monitoring programs, and the level of nitro- and oxy-PAHs in the Arctic atmosphere is unknown (Balmer and Muir, 2017).

The Arctic is warming at a higher rate than the global average and visible changes happen rapidly here. Thus, it is a key area for modeling studies on climate effects on contaminants with a main focus on LRAT from lower latitudes. As a consequence, local Arctic sources are usually disregarded, and lack of information on local emission sources is a source of

65 uncertainty in model predictions that often deviate significantly from observations (Schmale et al., 2018). Local emission sources may be of high importance in winter, when strong temperature atmospheric inversions can be frequent in Arctic region (Bradley et al., 1992). These episodes inhibit the mass and heat fluxes from the surface to the atmosphere, and consequently the dilution of surface emissions (Janhall et al., 2006; Li et al., 2019). This trapping of emissions results in poor air quality and can be potentially harmful to local people. Climate change introduces additional sources of PAHs to the

70 Arctic region. In the past decade, human activities such as resource exploration, research, tourism, fisheries, and maritime traffic have increased substantially due to warming and corresponding reduction of sea ice, opening up new shipping routes (Jörundsdóttir et al., 2014). Warming may also enhance volatilization of low molecular weight (LMW) PAHs from ground surfaces (Friedman et al., 2014) and melting sea ice (Yu et al., 2019). Reactivity of PAHs in the gas phase is significantly greater than when associated with particles (Keyte et al., 2013), therefore increasing air temperatures can be expected to lead

75 to increased levels of toxic nitro- and oxy-PAHs.

The need for a comprehensive assessment of local contaminant sources in Svalbard was acknowledged and initiated in the international Arctic Monitoring and Assessment Programme (AMAP); with the major focus on persistent organic pollutants (Pedersen et al., 2011), there is a scarcity of data on local sources of PAHs in Svalbard. A back-trajectory analysis of twenty years data for thee representative PAHs (Phe, Pyr, and BaPyr; see Table 1 for full names) suggested that Svalbard is

80 impacted by air masses coming from eastern Russia, northern Europe, and northwest Russia during winter (Yu et al., 2019). Overall, combined European and Russian emissions accounted for more than 80% of episodic high-concentration events in Svalbard in 2007 (Balmer and Muir, 2017; Friedman and Selin, 2012). However, observed concentrations of Phe and Pyr from the Zeppelin station, Svalbard, were higher than model simulations, indicating important contributions of local sources

of PAHs to the Arctic atmosphere, too (Yu et al. (2019). This study focused on the main settlement in Svalbard,
85 Longyearbyen, with a population of approximately 2300 inhabitants and a high level of (partially seasonal) human activities
(transport, coal mining, industry, tourism, and research). The local coal-fired power plant (PP) was hypothesized to be the
major local source of PAHs, and the overall objectives of this study were to: (1) evaluate PAH emissions from the local
power plant, (2) examine concentrations and profile changes with distance from the PP, (3) quantify concentrations of PAHs
and nitro- and oxy-PAHs, in both gaseous and particulate phases, and (4) determine other potential local sources of PAHs,
90 and nitro- and oxy-PAHs.

2 Material and methods

2.1 Sampling site

Svalbard is an archipelago located between latitudes 77° and 81°N in the Western Barents Sea. Longyearbyen, being the
largest populated settlement, was chosen as the study area. The local PP was installed in Longyearbyen in the 1980s and
95 provides the community with sufficient electricity (45 000 MW) and central heating supply (70 000 MW) throughout the
year (Bøckman, 2019). The PP is fueled by coal produced in a nearby mine at Breinosa (mine No. 7). This coal has a distinct
quality (brown, high volatile bituminous coal with vitrinite reflectance R_o=0.78% (Marshall et al., 2015)) and is well suited
for energy production. Coal consumption is about 25-30 thousand ton per year. The PP has two boilers, 32 MW each. The
coal burning temperature is about 1000 °C (Bøckman, 2019). Since December 2015, the flue gas purification system consists
100 of a selective non-catalytic reduction (SNCR) system, an electrostatic precipitator (ESP), and a wet flue-gas desulfurization
(WFGD) scrubber. After SNCR the NO_x content in the flue gas is reduced by 50% by spraying urea solution as a reduction
agent into the boiler. Further, in the ESP step, dust is electrically charged and deflected toward the collection electrodes. In
the WFGD scrubber, the flue gas is cooled and desulfurized by sea water.

For PP emission analysis, stack emission air samples were collected at source (PP), and two locations at transect distance:
105 the roof of the University Centre in Svalbard (UNIS, urban location, 1 km from PP) and the former northern lights
observatory in Adventdalen (Adventdalen, rural location, 6 km from PP, 7 km to the active coal mine No. 7) (Fig. 1).
Sampling at UNIS and Adventdalen was performed simultaneously.

2.2 Sample collection

2.2.1 Power plant

110 A total of 6 low volume (1.3-3.0 m^3) samples of the PP stack emission were collected (Table S1) under normal operating
conditions, collected on 27th September (PP1-PP3) and 2nd October (PP4-PP6) 2018. Sampling was performed downstream
the scrubber, after all flue gas cleaning steps. The sampling probe (inner Ø = 11 mm) was situated to face the direction of the
flue gas. A custom-made low volume, battery powered, air sampler (Digitel, Switzerland) was used to pump the flue gas
through the sampling material placed in a stainless steel cartridge (16249, Sartorius Stedim Biotech GmbH, Germany). The
115 particulate phase was collected on quartz fiber filter (QFF, pre-burned at 450°C for 6 h; Ø = 47 mm, Pallflex, USA), and the
gaseous phase on polyurethane foam (PUF, pre-cleaned in toluene for 24 h followed by 24 h acetone wash; Ø = 50 mm, L =
75 mm, Klaus Ziemer GmbH, Germany). Although, the pump was operated at the maximum speed (35 L min^{-1}, which
corresponds to 6.1 m s^{-1} probe intake flow speed), an isokinetic sampling regime was not achieved. The flue gas parameters
(temperature 8.9±0.5°C, moisture 28±2%, flow speed 18.1±0.8 m s^{-1}, and density 1.24±0.2 kg m^{-3}) were measured during the
120 sampling by FKT3DP1A multi meter equipped with S-type Pitote probe (FlowKinetics LLC, USA).

2.2.2 UNIS and Adventdalen

The prevailing wind direction in Longyearbyen and Adventdalen is from the southeast. In summer, when the soil surface in Adventdalen becomes warmer than water surface in Adventfjørd, the wind direction can temporary change to northwesterly. To focus on PP emission and avoid the peak marine traffic in the summer, simultaneous sampling at UNIS and Adventdalen was carried out from 28th August to 28th of September 2018 (Table S1), on days with predicted northwesterly wind direction, using high volume air samplers (TISCH-1000-BLXZ, TISCH Environmental Inc., USA) equipped with dual chamber sampling module (particle filter, stainless screen and vapor filter, glass cartridge). About 370 m[3] of ambient air was collected over 24 h per sample (Table S1). For each station, 6 high volume air samples were collected for particulate (QFF, pre-burned at 450°C for 6 h; Ø = 103 mm, Munktell/Ahlstrom, Finland) and gaseous (PUF, pre-cleaned in toluene for 24 h followed by 24 h acetone wash; Ø = 65 mm, L = 100 mm, Klaus Ziemer GmbH, Germany) phases. Weather parameters including ambient temperature, relative humidity, UV radiation, wind direction, and precipitation were recorded (Table S2). All samples were kept intact inside the sampling unit after collection. In order to reduce the risk of post-collection contamination, the unit was sealed in two plastic bags for transportation to the lab, where samples were removed from the unit, sealed with layers of aluminum foil, and stored airtight in two plastic bags. Samples were kept frozen at -20°C until analyzed. A total of 18 samples (18 QFFs and 18 PUFs) and 8 field blanks (4 for PP and 4 for UNIS and Adventdalen) were collected.

2.3 Analytical procedure

16 PAHs, 8 oxy- and 21 nitro-PAHs (Table S3) were quantified using GC-EI-MS/MS and GC-ECNI-MS, respectively. Full details on analytical methods, including equipment and procedures, are outlined in the SI (Text S1, Tables S4 and S5). In brief, all QFFs (particulate phase) and PUFs (gaseous phase) samples were extracted separately by two different methods, followed by the same clean-up procedure. Several ^{2}H-labelled PAH (dPAH) surrogates (16 dPAHs, 3 dOxy-PAHs, and 6 dNitro-PAHs), were added to samples prior to extraction. QFF samples were extracted with dichloromethane using QuEChERS-like procedure developed previously for the analysis of particulate bound PAHs (Albinet et al., 2013; Albinet et al., 2014). PUF samples were Soxhlet extracted with dichloromethane for 24 h. The extracts were concentrated and cleaned up first with neutral alumina Al_2O_3, and then with neutral silica SiO_2. Elutes were dried under gentle nitrogen stream and redissolved in approximately 100 μL n-hexane. The purified samples were spiked with three labelled standards to evaluate the surrogate recoveries.

2.4 Quality assurance

Detailed information on method validation and quality control is provided in SI (Text S2). Field (n=4 for PP, n=4 for UNIS and Adventdalen combined) and laboratory (n=3 for PP, n=3 for UNIS and Adventdalen combined) blanks were analysed in order to evaluate possible contamination during sample transport and analysis. The method detection limit (MDL) was determined based on blank values for each sampling material type (Table S6). High contamination of PUF blank samples by 9,10-PheQ (for UNIS and Adventdalen), and 2-NFlu (for PP) was found; these compounds were excluded from the final results. No blank correction was performed for the concentration calculations. Samples with PAH concentrations below instrumental limit of quantification (LOQ) were replaced by LOQ/2 for statistical analysis. The method efficiency was tested using QFF (n=4) and PUF (n=4) spiked samples (Table S7). Acceptable recoveries ranged between 63-109% for dPAHs, 56-68% for dOxy-PAHs, and 44-89% for dNitro-PAHs (Table S8).

2.5 Statistical analysis

Statistical analyses of compound concentrations were performed with Minitab 18 Statistical Software (Minitab LLC, Pennsylvania, USA). Normality and homogeneity of variances were tested with Shapiro-Wilk and Levene's tests,

respectively. Mann–Whitney U test was performed to test significant differences between sampling locations (UNIS and Adventdalen). Spearman's correlation was used to investigate relationships between different variables. The statistical significance was set at $p < 0.05$, unless stated.

Principle component analysis (PCA) was performed for PAH source apportionment. A 6×29 matrix (sample number × 29 detected compounds, including 14 PAHs and 15 nitro- and oxy-PAHs) dataset was used to assess the source contribution to PAHs for each location, and 12×29 matrix dataset to investigate PAH profile differences between UNIS and Adventdalen. Total PAH concentrations (gaseous and particulate, G+P), were used to minimize the influence of partitioning, ageing, and photochemical degradation (Kim et al., 2009). PCA was based on a correlation matrix to standardize scales and weight all variables equally (Holmes et al., 2017). PCA was first applied on the concentrations matrix only, and then weather parameters were carefully included in order to explain the observed sample groupings.

3 Results and discussion

3.1 Longyearbyen power plant PAH emission profile

Individual concentrations and phase distribution (percentage on particulate matter, %PM) of target PAH are summarized in Table 1. The sum of total (G+P) concentration of the 16 priority PAHs ($\sum$16 PAHs; U.S. Environmental Protection Agency) in the purified flue gases emitted from the PP is 0.106 µg m^{-3}, which corresponds to 1.5 µg kg^{-1} coal. Currently, there is no PAH emissions standard for coal-fired power plants in Norway. However, compared to the Canadian emission limits of PAHs for municipal solid waste incinerators of 5 µg m^{-3} (Li et al., 2016), the Longyearbyen PP emissions is a factor of 3 lower. About 94% of 16 PAHs were emitted in a gas phase, in agreement with earlier studies (Li et al., 2016; Wang et al., 2015; Yang et al., 1998). The emission profile of the Longyearbyen PP is dominated by LMW PAHs (2 and 3 rings), which represents 89% of $\sum$16 PAHs emission; high molecular weight (HMW) PAHs (5-7 rings) were not detected, likely due to their low vapor pressure and thus association to particles. A combination of ESP and WFGD has a removal efficiency of PM up to 99.9% (Wang et al., 2019). Fine cooling of the PP flue gas (8.9 ± 0.5 °C) by cold sea water facilitates high PM collection efficiency as well (Noda and Makino, 2010; Wang et al., 2019). As a result, PP dust emissions are below the ultra-low standard of 5 mg m^{-3} (Zhao et al., 2017) at 1.5 ± 0.2 mg m^{-3} (Lundgjerdingen, 2017). The PAH emissions profile was dominated by Nap and Phe, accounting for 53 % and 27 % of $\sum$16 PAHs, followed by Flu, Flt and Pyr. Nap and Phe are often reported as major emitted compounds from power plants equipped with analogous exhaust cleaning systems and/or burning the same type of coal (Hsu et al., 2016; Li et al., 2016; Wang et al., 2015). A similar PAH emissions profile was reported by Hsu et al. (2016) for the power plant in central Taiwan (Table S12). A higher flue gas dust concentration and different coal sources resulted in 40% emissions of four ringed PAHs compared to 11% for Longyearbyen PP. Operation conditions and boiler type can have significant effects on emitted PAH profiles and concentrations (Wang et al., 2015), as well as combustion temperature (Peng et al., 2016), and geological maturity (Huang et al., 2014b).

Nitro- and oxy-PAHs are constituents of raw coal and can also be produced from parent PAH compounds during high temperature coal combustion (Huang et al., 2014b). The yields of individual nitro-PAHs from the PP was 1 - 2 orders of magnitude lower than those of their corresponding parent PAHs, and individual concentrations were at or below 1.7 ng m^{-3}; 1-NNap was the most abundant nitro-PAH. Huang et al. (2014b) investigated the same type of coal (bituminous, $R_0 = 0.77$ %), burned at lower temperatures in a honeycomb briquette stove; nitro-PAHs were absent in the raw coal and calculated nitro-PAH/PAH ratios were >1 confirming formation of nitro-PAH compounds during coal combustion. In contrast, in the present work, the same daughter to parent PAH ratios were < 1 (Table 2), indicating an absence of nitro-PAH formation during coal combustion or possible thermal degradation of nitro-PAH at 1000 °C.

The yields of oxy-PAHs were orders of magnitude higher than nitro-PAHs because oxy-PAHs can be produced by reaction of PAH with O˙ or ˙OH radicals generated continuously by radical chain reactions during combustion (Huang et al., 2014b).

9-Flu and 9,10-AntQ were the most abundant among the oxy-PAHs (12.4 and 15.6 ng m^{-3}, respectively), and concentration of 9,10-PheQ was a factor of six lower. The calculated ratios of oxy-PAH to corresponding parent PAH were lowest for 9,10-PheQ/Phe and highest for 9,10-AntQ/Ant (Table 2). This can be due to a higher content of Phe in coal, as well as
205 different reaction rates of Phe, Ant, and Flu with O˙ or ˙OH radicals. Difference between the reaction rates of Flu and Ant can possibly be explained by different reaction pathways; Flu undergoes H atom abstraction at the 9-position to form 9-Flu, while Ant requires ˙OH attack on the aromatic ring (Brubaker and Hites, 1998). Ant and Phe have essentially the same 3-ring structure, only differing by the relative position of their aromatic rings. However, Ant appears to be significantly more reactive, due to the sterically unhindered molecular structure of Ant (Keyte et al., 2013). Formation of specific PAHs is also
210 a temperature dependent process (Peng et al., 2016).

Ant, BaAnt, and Chry are often used as tracers of coal combustions (Zheng et al., 2019; Wu et al., 2014; Wang et al., 2009), however, their concentrations in the flue gas of the Longyearbyen PP were negligible. This demonstrates the strong importance of determining indicatory PAH profiles for individual combustion sources for correct source identification. PAH emissions from different coal plants are hard to compare because they are affected by many factors including coal type,
215 boiler load, combustion mode (Wang et al., 2015), and flue gas cleaning systems. Nap was the most abundant PAH emitted from the Longyearbyen PP. Nap is not a common tracer due to its ubiquitous presence and often high blank sampling material contamination; thus, Nap was not considered as potential marker. Further, Phe, Flu, Flt, Pyr, 9-Flu, and 9,10-AntQ were the main PAHs detected in the Longyearbyen PP flue gas (Fig. 2), therefore the presence and diagnostic ratios (Table 3) of these compounds were used as markers of the PP source in the present work. In Yu et al. (2019), coal combustion was
220 identified as the main source (68% contribution) of PAHs, at the Zeppelin monitoring station at Ny-Ålesund, Svalbard, and Phe, Flu, Flt, and Pyr were the main contributors, most likely attributable to the Longyearbyen PP located 115 km southeast of Ny-Ålesund. Overall, total flue gas emissions were 960 000 Nm^3 day^{-1} (Lundgjerdingen, 2017), and a daily emissions of Σ16 PAHs and sum of the nitro- and oxy-PAHs are approximately 98.7 g of and 35.6 g, respectively.

3.2 UNIS and Adventdalen

225 **3.2.1 Ambient concentrations and PAH profiles**

The concentrations of PAHs measured at UNIS was a factor of 2 higher than at Adventdalen, while the PAH profiles were similar. Σ16 PAHs was 749.2±72.6 and 369.1±66.7 pg m^{-3} at UNIS and Adventdalen, respectively (Table 1). ΣOxy-PAHs were approximately a factor of 2 lower, with average values of 471.0±150.8 (UNIS) and 233.1±68.3 pg m^{-3} (Adventdalen); Σnitro-PAHs were an order of magnitude lower than both parent PAHs and oxy-PAHs, with average values of 36.8±6.2
230 (UNIS) and 27.2±11.1 pg m^{-3} (Adventdalen). Among the parent PAHs, Phe (ranged from 191.7 to 470.0 pg m^{-3}) and Flu (ranged from 38.5 to 236.0 pg m^{-3}) were the most abundant at both sites. The PAH concentrations measured at Longyearbyen (UNIS and Adventdalen) were two orders of magnitude higher than those detected at the Zeppelin station and the same order of magnitude as in Birkenes (southern mainland Norway) (NILU, 2019) (Table S13) for the same period (autumn 2018). Phe and Flu also dominated the PAH profile at Zeppelin station, which may indicate similar sources of
235 contamination.

Concentrations of 9-Flu and 9,10-AntQ were the highest among measured oxy-PAHs in the present study. The 9-Flu level (270.3±146.9 pg m^{-3} at UNIS and 139.4±24.9 pg m^{-3} in Adventdalen) was the same order of magnitude as reported for the background monitoring stations in the north of Finland (Pallas) and in the south of Sweden (Råö) (Brorström-Lundén et al., 2010), while 9,10-AntQ (163.5±57.4 pg m^{-3} at UNIS and 71.7±39.2 pg m^{-3} in Adventdalen) was an order of magnitude
240 higher in Longyearbyen. The nitro-PAH levels in our study were overall lower than other reported background sites. 1-NNap and 2+3-NFlt were the most abundant nitro-PAHs detected at UNIS and Adventdalen air samples; the level of 2+3-NFlt (9.5±1.6 pg m^{-3} at UNIS and 12.3±7.7 pg m^{-3} in Adventdalen) was an order of magnitude higher than that at Råö and Pallas stations; 1-NNap average detected concentrations were 17.0±3.0 pg m^{-3} at UNIS and 5.0±3.2 pg m^{-3} in Adventdalen.

3.2.2 Gas/particle partitioning

245   Gas/particle partitioning is an important process that controls transport, degradation, and distribution patterns of contaminants in and between environmental compartments (Huang et al., 2014a). The sampling campaign in the present study was conducted from late Arctic summer until early autumn and during this period the temperature varied from 6.8 °C in August to -4.4°C in September and several precipitation events (snow and rain) occurred. In general, LMW PAHs were found in the gas phase, while HMW PAHs were present in the particulate phase (Table 1), which is in accordance to their

250   physico-chemical parameters, such as octanol-air partition coefficient (Table S3). Repartitioning between phases (Fig. 3) mainly impacted semi-volatile compounds with three and four aromatic rings (Flt, Pyr, BaAnt, Chry; 2-NFlu, 9-Flu, cPPhe-4, 9,10-AntQ, 9-NAnt, and 2+3-NFlt) as a response to changing meteorological conditions (Hu et al., 2019). Strong negative correlations (Spearman coefficient > 0.65) of percentage of PAH determined in particulate phase (%PM) with ambient temperature and specific humidity were determined for Chry, 1-NNap, 2-NNap, cPPhe-4, and 2+3-NFlt, although they were

255   not statistically significant (Table S14). Likely, it was confounded by diurnal variations in the rate of PAH emissions from different local sources. Specific humidity played an essential role in PAH wet scavenging as it is further discussed in Section 4.1.

Compared to Adventdalen, the urban UNIS location ensure a higher level of PAHs emitted from different nearby anthropogenic sources, including the PP. Low ambient temperature reinforces partitioning of freshly emitted gaseous PAHs

260   to the particulate phase. As a result, %PM at UNIS was higher than in Adventdalen. Deposition (wet and dry) and chemical reactions with atmospheric oxidants are important removal processes of PAH from air (Keyte et al., 2013). On the local scale, within an hour of travel time from PP to Adventdalen, it is not expected that photolytically-initiated transformation of the freshly emitted PAHs has a strong influence on gas phase concentrations and consequently on %PM. Dry deposition rates vary depending on the type of adsorbing particle (mass, size, aerodynamic properties, shape, and chemical

265   composition) and the atmospheric conditions (Weinbruch et al., 2018). The influence of wet deposition was indicated by a significant negative correlation between concentrations of several HMW PAHs (Pyr, Chry, BbkFlt, IPyr, BPer, BaFlu-11, and BaAnt-7,12) and precipitation (Spearman correlation, p<0.05, Table S15), resulting in a lower amount of particle-bound PAHs transported from the town, and thus lower %PM in Adventdalen.

4 Source identification

270   PCA was the main tool applied on Adventdalen (n=6) and UNIS (n=6) samples to determine possible PAH sources at each location, as well as on all the analyzed ambient samples together (n=12) to identify the difference between the two transect locations. Total PAH (G+P) concentrations were used to minimize the influence of partitioning, aging, and photochemical degradation. PAH diagnostic ratios (Table 4) were utilized as an additional supportive tool taking into account their possible shift due to large scale mixing of PAHs in the atmosphere, different emission rates of PAH from the same source, influence of changing environmental conditions (Katsoyiannis and Breivik, 2014), and atmospheric processing (Alam et al., 2013).

275   Transport of PAHs over short distances from a source can be enough to cause a change in interpretation and identification of the source (Katsoyiannis and Breivik, 2014). Different PAHs have diverse reactivity with other atmospheric species and half-lives in the atmosphere (Ravindra et al., 2008; Tobiszewski and Namieśnik, 2012). Due to high atmospheric reactivity of Ant and BaAnt, utilization as source apportionment should be avoided, while HMW PAH diagnostic ratios may be

280   exploited with greater confidence owing to their increased stability (Alam et al., 2013). Although, based on similarities in characteristic travel distances among pairs of PAHs, Katsoyiannis and Breivik (2014) named BaAnt/(BaAnt+Chry) ratio as the most robust for air concentrations. Conclusions on the chosen diagnostic ratios are incorporated in the PCA findings discussion. Two principal components (PCs) for Adventdalen (79%) and three PCs for UNIS (80%) were studied in details.

4.1 Adventdalen

285 Two PCs explain 79% of the total variance (Table S16) of Adventdalen data. PC1 (55%) revealed a distinct profile dependence on ambient conditions (temperature, specific humidity, and UV radiation). Two groups, "humid samples" (A1, A2, A3) and "dry samples" (A4, A5, A7), were identified (Fig. 4). The first group corresponds to the sampling days with higher values of temperature, specific humidity, and UV radiation (Table S2). Most of the target compounds in the "humid samples" were at lower concentrations compared to the "dry samples". The majority of PAHs were negatively correlated

290 with specific humidity, temperature, UV radiation, and precipitation (Fig. 4). Samples A2 and A5, corresponding to two days with heavy precipitation events (raining at +5 °C and snowing at -3 °C, respectively), were not grouped together but sharply separated by the PC1. This indicates that the mass of water vapor in the air (specific humidity), in contrast to relative humidity, is an essential parameter for removal from the atmosphere. In the present study, many compounds were negatively correlated with humid conditions, particularly the intense rainfall episode (sample A2, Fig. 4). Heavier molecular weight

295 compounds of this group (Chry, 9,10-AntQ, cPPhe-4, 9-NPhe, BaFlu-11, and BaAnt-7,12), which have lower vapor pressure and thus volatility, were full or partly bound to particles, 38-100% PM (Table 1). Therefore, they were readily scavenged by precipitation (rainfall). For those which are lighter and more volatile, water solubility (for Ace, Acy, Flu, Phe, 1- and 2-NNap, 9-Flu, and 9,10-AntQ) and polarity (for nitro- and oxy-PAHs) play an additional role in wet scavenging processes (Shahpoury et al., 2018). The gas phase removal from the atmosphere is due to substance dissolution in water droplets

300 (Shahpoury et al., 2018), which enhances the scavenging effect at higher humidity. A strong negative correlation with humidity was determined for all quantified LMW PAHs, significant for Acy, Pyr, 1-NNap, and 9-Flu (Spearman correlation, $p<0.05$; Table S17). Presence of Ant and Flt (gas-phase PAHs with low polarity and water solubility) in the group is likely due to the same source of origin.

Based on the tracers and their loadings (Table S16), PC1 can be assigned to local PP coal burning (Flu, Phe, Flt, Pyr, 9-Flu,

305 9,10-AntQ) and vehicular emissions (Pyr, Chry, 1-NNap, cPPhe-4, BaFlu-11, BaAnt-7,12). The diagnostic ratios IPyr/(IPyr+BPer) and IPyr/BPer indicated mainly contribution from diesel emissions (Table 4) and several of these compounds (cPPhe-4, 1-NNap, and BaAnt-7,12) were reported to be emitted after diesel burning as well (Rogge et al., 1993; Albinet et al., 2007; Zhao et al., 2018).

Besides, PC1 emphasized positive correlation of 2+3-NFlt and 9-NAnt with temperature, humidity, and UV radiation, as

310 well as negative correlation with a group of primary PAHs (Fig. 4, Table S17), suggestive of a secondary source of origin. The daughter to parent PAH ratios, 9-NAnt/Ant and 2+3-NFlt/Flt (Table S18), showed statistically significant correlations with temperature, humidity, and UV radiation (Spearman correlation, $p<0.10$; Table S19). Moreover, 2+3-NFlt and 9-NAnt had a strong positive correlation with each other and negatively correlated with their parent compounds (Spearman correlation, Table S20), by reason of assumed chemical transformation. It should be noted that 9-NAnt and 2+3-NFlt were

315 detected in the PP flue gas at low levels (0.08 ng/m^3 and 0.5 ng/m^3, respectively), and further statistical analysis (Spearman correlation, Table S20, Fig. 4) showed no correlation with established PP tracers (Phe, 9,10-AntQ, 9-Flu), suggesting a different source of origin. These results indicate atmospheric formation as an additional source of 9-NAnt and 2+3-NFlt, in agreement with other studies (Lin et al., 2015b; Hayakawa et al., 2000; Shahpoury et al., 2018). Sampling close to a major source of NO_x emission, such as the local power plant, can result in concentrations of NO_3 and NO_2 at high enough level for

320 atmospheric transformation of PAHs to occur. Relative contribution of primary and secondary sources of nitro-PAHs could be tested by applying a 2-NFlt/1-NPyr ratio (Zielinska et al., 1989), but 1-NPyr was not detected in our study. We conclude that PC1 (55%) is associated with local PP coal burning, atmospheric transformation, and traffic emission (mainly diesel exhaust) sources.

PC2 did not reveal additional PAH sources and confirmed inputs from the PP coal burning (Phe, Flu, and 9-Flu) and diesel

325 exhaust (4-NBip, 1- and 2-NNap, 2+3-NFlt, Hu et al., 2013; Keyte et al., 2013; Alam et al., 2015). Moreover, PC2 revealed a negative correlation of LMW PAHs, namely 4-NBip, 2-NNap, Phe, Flu, 1-NNap, 9-Flu, and Acy (in loading order) with

precipitation, mainly snow on day five (sample A5, Fig. 4). These PAHs were detected in the gas-phase. Commonly, wet scavenging of PAHs is considered to be ineffective, unless the substance is particle-associated (Škrdlíková et al., 2011). However, studies by Wania et al. (1999) report that snow scavenging may be an important, and sometimes a dominating

330   scavenging process for lighter PAHs, mediated via a process of adsorption to the air-ice (Wania et al., 1999).

The two PCs explain 79% of the total variance. Traffic emission (mainly diesel exhaust) and the Longyearbyen coal-burning PP were the main local sources of PAHs and nitro- and oxy-PAHs in Adventdalen, and atmospheric transformation of PAHs is an additional source of nitro-PAHs. The statistical analysis has also emphasized the importance of weather conditions on the spatial distribution and concentrations of PAHs. LMW PAHs were scavenged by snow, while the level of humidity was

335   an essential parameter for total PAH removal from the atmosphere.

4.2 UNIS

The UNIS sampling location is only 1 km away from the local coal-fired PP and the PAH profile is therefore influenced by local activities in and around the town. Three PCs explain 80.3% of the total variance (Table S21). PC1 (41%) was equally loaded with Flt, Pyr, BaAnt, Chry, BbkFlt, BaPyr, IPyr, BPer, 2-NNap, BaAnt-7,12, BaFlu-11, and BZT, which are

340   commonly found in traffic emissions. The diagnostic ratios IPyr/(IPyr+BPer) and IPyr/BPer mainly indicated contribution from gasoline emissions (Table 4) and several of these compounds (BPer, IPyr, and BaFlu-11) were reported to be emitted after gasoline burning as well (Zielinska et al., 2004; Albinet et al., 2007). Absence of 1-NPyr and 2-NFlu, the principal compounds of diesel exhaust (Albinet et al., 2007), supported gasoline combustion as more dominant source as well. Precipitation data was included in PCA as variables to explain sample groupings. On the PC1 biplot (Fig. 5) samples U1, U2,

345   and U5, collected on days with substantial precipitation (snow and rain; Table S2), are grouped together. All PC1 contributors showed negative correlations with precipitation. For Pyr, Chry, BbkFlt, BPer, and BaAnt-7,12 the negative correlation with precipitation was statistically significant (Spearman correlation, $p<0.10$; Table S15). The majority of these PAH derivatives were found mainly in the particulate fraction (Table 1), and lighter compounds were less affected by precipitation. This is in agreement with particle scavenging dominant during wet deposition (Škrdlíková et al., 2011). Zhang

350   et al. (2015) reported that scavenging of particulate-phase PAHs is about 20 times more efficient than scavenging of gas-phase PAHs.

PC2 (25%) was highly loaded by wind direction (Fig. 5, Table S21), and samples were split between two groups depending on prevailing wind direction during sampling. The first group was characterized by the presence of 9,10-AntQ, Phe, and Flu, attributable to the PP emission source. Diagnostic ratios of Flu/(Flu+Pyr) and BaAnt/(BaAnt+Chry) (Table 4) also indicated

355   that the PP is a source of PAHs and nitro- and oxy-PAHs at UNIS. 9-Flu, a tracer for the PP, may have other possible sources, including diesel and gasoline vehicle exhaust, coal powder, road dust particles (Keyte et al., 2013), and may be locally produced, transported from longer range, or secondarily formed in the atmosphere (Kojima et al., 2010). 9-Flu is associated with the second sample grouping (U2, U6, U7), collected during conditions of wind blowing from the west and west southwest (Fig. S1), and they are characterized by the presence of 4-NBip, 1,5-DNNap, 2+3-NFlt, and 2-NFlu, known

360   markers for diesel emissions (Hu et al., 2013; Keyte et al., 2013; Helmig et al., 1992). This can be explained by coal transportation by trucks, mining work, geotechnical drilling, and boat traffic in the fjord. Therefore, PC2 was attributed to coal burning emissions from the PP and diesel emissions.

PC3 (15%) was loaded mainly with 9-NAnt, cPPhe-4, 9-Flu, and 2+3-NFlt (Table S21). These compounds may originate from combustion processes, often from vehicle emissions. However, on the PC3 score and loading plots (Fig. S2) it can be

365   interpreted that these compounds were negatively correlated with other traffic emission tracers such as 1-NNap, 2-NNap, BZT, 2- and 4-NBip, and BaFlu, suggesting different sources of origin. Several studies have shown that 9-NAnt, cPPhe-4, 9-Flu, and 2+3-NFlt can be secondarily formed via chemical reactions in the atmosphere (Singh et al., 2017; Lin et al., 2015a; Zhao et al., 2018). The compounds were also associated with the sample U2, collected on the warmest day with high UV

radiation and humidity levels. Thus, a secondary origin of 9-NAnt and 2+3-NFlt at UNIS was concluded, in agreement with

370   source apportionment in Adventdalen, and PC3 was attributed to atmospheric transformation of PAHs.

The three PCs explain 79.7% of the total variance of the UNIS samples. PP coal burning, gasoline and diesel emissions, and atmospheric transformations were determined as the main sources of PAHs and nitro- and oxy-PAHs at UNIS.

4.3 Transect ambient samples

PCA was performed to compare samples collected at UNIS and Adventdalen locations (n=12; Fig. 6). The same potential

375   sources of PAHs and nitro- and oxy-PAHs for the Longyearbyen-Adventdalen vicinity were confirmed, which explains their similar profiles. Samples from UNIS and Adventdalen were clearly separated due to the higher concentrations of almost all the detected compounds at UNIS, originating from Longyearbyen activities: coal combustion in the PP, vehicle traffic, and marine traffic. LRAT input, including secondary formation of the derivatives, was more evident in Adventdalen where town emissions influence is reduced. In contrast to the study by Yu et al. (2019), no strong indication for LRAT biomass burning

380   emissions was found for this set of air samples.

5 Conclusion

Results provide insights into local sources of atmospheric PAHs and nitro- and oxy-PAHs in Svalbard. Source markers for the coal-burning PP in Longyearbyen were determined, and generally low emissions of PAHs confirmed an efficient exhaust cleaning system. However, PAHs are emitted daily from coal-burning, and due to a large volume of flue gas emissions, the

385   PP remains an important local anthropogenic source of atmospheric contaminants. Ambient air concentrations of PAHs were substantially affected by rain and snow, and specific humidity plays an important role in PAH removal from the atmosphere. Overall, PAH concentrations were the same order of magnitude as detected at other background Scandinavian air sampling stations. The gas/particle partitioning of PAHs and nitro- and oxy-PAHs was dependent on air temperature and specific humidity, and mainly impacted semi-volatile compounds with three and four aromatic rings. Traffic emissions was another

390   contributor to PAH emissions, with larger input from gasoline-driven cars at UNIS and diesel vehicles at the remote site due to mining and geotechnical work in Adventdalen. The results also revealed secondary atmospheric formation as an additional source of some nitro-PAHs. The present study contributes to understanding fate and distribution of PAHs in the Arctic, and it provides important information on the phase-separated concentrations of PAHs, and nitro- and oxy-PAHs in Arctic air, as well as markers of the Longyearbyen PP emissions. This data can eliminate uncertainties in model predictions that aim to

395   assess the extent and impacts of Arctic atmospheric contaminants. Furthermore, the knowledge on the local emissions level can be important in case of temperature inversion in the lower atmosphere when vertical dilution is limited and contaminants are trapped near the ground, which may be adverse to public health.

Data availability. The dataset used in this paper is included in the Supplement, and further information is available from the

400   corresponding author tatiana.drotikova@unis.no.

Supplement. The supplement related to this article is available online at: xxx.

Author contribution. RK, AKH, and HR designed the campaign. TD conducted the field and lab works. TD with support

405   from AA and RK optimized, validated and performed GC analysis and further quantification. TD processed and interpreted PCA outcome. TD prepared the manuscript with contributions from all co-authors. TD, AA, and AKH prepared the Supplementary materials section.

Competing interests. The authors declare that there is no conflict of interest.

410

Acknowledgements. We gratefully acknowledge Longyearbyen Lokalstyre (Longyearbyen Community Council), personally Kim Rune Røkenes (a former leader of Energyverket), for the support on performing the PP exhaust sampling. We also thank Rasmus Bøckman (Lokalstyre, Energyverket) for providing information on the PP system operating parameters; Morten Hogsnes and Kristin Lundgjerdingen (Applica Test & Certification AS) for sharing their knowledge on PP flue gas

415 sampling; Siiri Wickström (UNIS) for helping with weather prediction; Marcos Porcires (UNIS) for on-site installation of weather station; Øyvind Mikkelsen (Norwegian University of Science and Technology) for teaching on PCA topic; Malte Jochmann (UNIS/Store Norske) for fruitful discussions on Svalbard coal quality. This research was financially supported by UNIS, NMBU, and the Svalbard Environmental Protection Fund (AtmoPart project).

References

420

Akyüz, M., and Çabuk, H.: Gas–particle partitioning and seasonal variation of polycyclic aromatic hydrocarbons in the atmosphere of Zonguldak, Turkey, Sci. Total Environ., 408, 5550-5558, https://doi.org/10.1016/j.scitotenv.2010.07.063, 2010.

Alam, M. S., Delgado-Saborit, J. M., Stark, C., and Harrison, R. M.: Using atmospheric measurements of PAH and quinone

425 compounds at roadside and urban background sites to assess sources and reactivity, Atmos. Environ., 77, 24-35, https://doi.org/10.1016/j.atmosenv.2013.04.068, 2013.

Alam, M. S., Keyte, I. J., Yin, J., Stark, C., Jones, A. M., and Harrison, R. M.: Diurnal variability of polycyclic aromatic compound (PAC) concentrations: Relationship with meteorological conditions and inferred sources, Atmos. Environ., 122, 427-438, https://doi.org/10.1016/j.atmosenv.2015.09.050, 2015.

430 Albinet, A., Leoz-Garziandia, E., Budzinski, H., and Viilenave, E.: Polycyclic aromatic hydrocarbons (PAHs), nitrated PAHs and oxygenated PAHs in ambient air of the Marseilles area (South of France): Concentrations and sources, Sci. Total Environ., 384, 280-292, https://doi.org/10.1016/j.scitotenv.2007.04.028, 2007.

Albinet, A., Tomaz, S., and Lestremau, F.: A really quick easy cheap effective rugged and safe (QuEChERS) extraction procedure for the analysis of particle-bound PAHs in ambient air and emission samples, Sci. Total Environ., 450-451,

435 31-38, https://doi.org/10.1016/j.scitotenv.2013.01.068, 2013.

Albinet, A., Nalin, F., Tomaz, S., Beaumont, J., and Lestremau, F.: A simple QuEChERS-like extraction approach for molecular chemical characterization of organic aerosols: application to nitrated and oxygenated PAH derivatives (NPAH and OPAH) quantified by GC–NICIMS, Anal. Bioanal.Chem., 406, 3131-3148, https://doi.org/10.1007/s00216-014-7760-5, 2014.

440 Armitage, J. M., Quinn, C. L., and Wania, F.: Global climate change and contaminants-an overview of opportunities and priorities for modelling the potential implications for long-term human exposure to organic compounds in the Arctic, J Environ Monit, 13, 1532-1546, https://doi.org/10.1039/c1em10131e, 2011.

Balmer, J., and Muir, D.: Polycyclic aromatic hydrocarbons (PAHs), in: AMAP Assessment 2016: Chemicals of emerging Arctic concern, edited by: Hung, H., Letcher, R., and Yu, Y., Arctic Monitoring and Assessment Programme

445 (AMAP), Oslo, Norway, 219-238, 2017.

Bandowe, B. A. M., and Meusel, H.: Nitrated polycyclic aromatic hydrocarbons (nitro-PAHs) in the environment – A review, Sci. Total Environ., 581-582, 237-257, https://doi.org/10.1016/J.SCITOTENV.2016.12.115, 2017.

Barrie, L. A., Gregor, D., Hargrave, B., Lake, R., Muir, D., Shearer, R., Tracey, B., and Bidleman, T.: Arctic contaminants: Sources, occurrence and pathways, Sci Total Environ, 122, 1-74, https://doi.org/10.1016/0048-9697(92)90245-n,

450 1992.

Bradley, R. S., Keimig, F. T., and Diaz, H. F.: Climatology of surface-based inversions in the North American Arctic, J. Geophys. Res., 97, 15699, https://doi.org/10.1029/92JD01451, 1992.

Brorström-Lundén, E., Remberger, M., Kaj, L., Hansson, K., Palm Cousins, A., and Andersson, H.: Results from the Swedish national screening programme 2008, IVL Swedish Environmental Research Institute, Göteborg, Sweden, 69,

455 2010.

Brubaker, W. W., and Hites, R. A.: OH reaction kinetics of polycyclic aromatic hydrocarbons and polychlorinated dibenzo-p-dioxins and dibenzofurans, J. Phys. Chem. A, 102, 915-921, https://doi.org/10.1021/jp9721199, 1998.

Bøckman, R.: Fremtidens energiutfordringer på Svalbard (in Norwegian), Longyearbyen Lokalstyre, Norway, Open file at www.uit.no, last access: 28 January 2020, 10, 2019.

460 Durant, J. L., Busby Jr, W. F., Lafleur, A. L., Penman, B. W., and Crespi, C. L.: Human cell mutagenicity of oxygenated, nitrated and unsubstituted polycyclic aromatic hydrocarbons associated with urban aerosols, Mutation Research/Genetic Toxicology, 371, 123-157, http://dx.doi.org/10.1016/S0165-1218(96)90103-2, 1996.

Fiedler, H., Kallenborn, R., Boer, J. d., and Sydnes, L. K.: The Stockholm Convention: A tool for the global regulation of persistent organic pollutants, Chem. Int., 41, 4-11, https://doi.org/10.1515/ci-2019-0202, 2019.

465   Friedman, C. L., and Selin, N. E.: Long-range atmospheric transport of polycyclic aromatic hydrocarbons: a global 3-D
           model analysis including evaluation of Arctic sources, Environ. Sci. Technol., 46, 9501-9510,
           https://doi.org/10.1021/es301904d, 2012.
       Friedman, C. L., Zhang, Y., and Selin, N. E.: Climate change and emissions impacts on atmospheric PAH transport to the
           Arctic, Environ. Sci. Technol., 48, 429-437, https://doi.org/10.1021/es403098w, 2014.
470   Fu, P., Kawamura, K., Chen, J., and Barrie, L. A.: Isoprene, monoterpene, and sesquiterpene oxidation products in the high
           Arctic aerosols during late winter to early summer, Environ. Sci. Technol., 43, 4022-4028,
           https://doi.org/10.1021/es803669a, 2009.
       Hayakawa, K., Murahashi, T., Akutsu, K., Kanda, T., Tang, N., Kakimoto, H., Toriba, A., and Kizu, R.: Comparison of
           polycyclic aromatic hydrocarbons and nitropolycyclic aromatic hydrocarbons in airborne and automobile exhaust
475   particulates, Polycyclic Aromat. Compd., 20, 179-190, https://doi.org/10.1080/10406630008034784, 2000.
       Helmig, D., Arey, J., Atkinson, R., Harger, W. P., and McElroy, P. A.: Products of the OH radical-initiated gas-phase
           reaction of fluorene in the presence of NOx, Atmos. Environ. A-Gen, 26, 1735-1745, https://doi.org/10.1016/0960-
           1686(92)90071-r, 1992.
       Holmes, D., Moody, P., Dine, D., and Trueman, L.: Research methods for the biosciences, Oxford University press, Oxford,
480   United Kingdom, 2017.
       Hsu, W. T., Liu, M. C., Hung, P. C., Chang, S. H., and Chang, M. B.: PAH emissions from coal combustion and waste
           incineration, J. Hazard. Mater., 318, 32-40, http://doi.org/10.1016/j.jhazmat.2016.06.038, 2016.
       Hu, H., Tian, M., Zhang, L., Yang, F., Peng, C., Chen, Y., Shi, G., Yao, X., Jiang, C., and Wang, J.: Sources and gas-particle
           partitioning of atmospheric parent, oxygenated, and nitrated polycyclic aromatic hydrocarbons in a humid city in
485   southwest China, Atmos. Environ., 206, 1-10, https://doi.org/10.1016/j.atmosenv.2019.02.041, 2019.
       Hu, S., Herner, J. D., Robertson, W., Kobayashi, R., Chang, M. C. O., Huang, S.-M., Zielinska, B., Kado, N., Collins, J. F.,
           Rieger, P., Huai, T., and Ayala, A.: Emissions of polycyclic aromatic hydrocarbons (PAHs) and nitro-PAHs from
           heavy-duty diesel vehicles with DPF and SCR, J. Air Waste MA, 63, 984-996,
           https://doi.org/10.1080/10962247.2013.795202, 2013.
490   Huang, B., Liu, M., Bi, X., Chaemfa, C., Ren, Z., Wang, X., Sheng, G., and Fu, J.: Phase distribution, sources and risk
           assessment of PAHs, NPAHs and OPAHs in a rural site of Pearl River Delta region, China, Atmos. Pollut. Res., 5,
           210-218, https://doi.org/10.5094/APR.2014.026, 2014a.
       Huang, W., Huang, B., Bi, X., Lin, Q., Liu, M., Ren, Z., Zhang, G., Wang, X., Sheng, G., and Fu, J.: Emission of PAHs,
           NPAHs and OPAHs from residential honeycomb coal briquette combustion, Energy & Fuels, 28, 636-642,
495   https://doi.org/10.1021/ef401901d, 2014b.
       Janhall, S., Olofson, K., Andersson, P., Pettersson, J., and Hallquist, M.: Evolution of the urban aerosol during winter
           temperature inversion episodes, Atmos. Environ., 40, 5355-5366, https://doi.org/10.1016/j.atmosenv.2006.04.051,
           2006.
       Jörundsdóttir, H. Ó., Jensen, S., Hylland, K., Holth, T. F., Gunnlaugsdóttir, H., Svavarsson, J., Ólafsdóttir, Á., El-Taliawy,
500   H., Rigét, F., Strand, J., Nyberg, E., Bignert, A., Hoydal, K. S., and Halldórsson, H. P.: Pristine Arctic: Background
           mapping of PAHs, PAH metabolites and inorganic trace elements in the North-Atlantic Arctic and sub-Arctic coastal
           environment, Sci. Total Environ., 493, 719-728, http://dx.doi.org/10.1016/j.scitotenv.2014.06.030, 2014.
       Katsoyiannis, A., and Breivik, K.: Model-based evaluation of the use of polycyclic aromatic hydrocarbons molecular
           diagnostic ratios as a source identification tool, Environ. Pollut., 184, 488-494,
505   https://doi.org/10.1016/j.envpol.2013.09.028, 2014.
       Kavouras, I. G., Koutrakis, P., Tsapakis, M., Lagoudaki, E., Stephanou, E. G., Von Baer, D., and Oyola, P.: Source
           apportionment of urban particulate aliphatic and polynuclear aromatic hydrocarbons (PAHs) using multivariate
           methods, Environ. Sci. Technol., 35, 2288-2294, https://doi.org/10.1021/es001540z, 2001.
       Keyte, I. J., Harrison, R. M., and Lammel, G.: Chemical reactivity and long-range transport potential of polycyclic aromatic
510   hydrocarbons – a review, Chem. Soc. Rev., 42, 9333-9391, https://doi.org/10.1039/C3CS60147A, 2013.
       Kielhorn, J., Wahnschaffe, U., and Mangelsdorf, I.: Environmental health criteria 229. Selected nitro- and nitro-oxy-
           polycyclic aromatic hydrocarbons, World Health Organization, 511 pp., 2003.
       Kim, D., Kumfer, B. M., Anastasio, C., Kennedy, I. M., and Young, T. M.: Environmental aging of polycyclic aromatic
           hydrocarbons on soot and its effect on source identification, Chemosphere, 76, 1075-1081,
515   https://doi.org/10.1016/j.chemosphere.2009.04.031, 2009.
       Kim, K.-H., Jahan, S. A., Kabir, E., and Brown, R. J. C.: A review of airborne polycyclic aromatic hydrocarbons (PAHs) and
           their human health effects, Environ. Int., 60, 71-80, https://doi.org/10.1016/j.envint.2013.07.019, 2013.
       Klonecki, A.: Seasonal changes in the transport of pollutants into the Arctic troposphere-model study, J. Geophys. Res., 108,
           http://doi.org/10.1029/2002jd002199, 2003.
520   Kojima, Y., Inazu, K., Hisamatsu, Y., Okochi, H., Baba, T., and Nagoya, T.: Influence of secondary formation on
           atmospheric occurrences of oxygenated polycyclic aromatic hydrocarbons in airborne particles, Atmos. Environ., 44,
           2873-2880, https://doi.org/10.1016/j.atmosenv.2010.04.048, 2010.
       Lammel, G.: Long-range atmospheric transport of polycyclic aromatic hydrocarbons is worldwide problem - results from
           measurements at remote sites and modelling, Acta Chimica Slovenica, 729-735,
525   https://doi.org/10.17344/acsi.2015.1387, 2015.
       Li, J., Li, X., Li, M., Lu, S., Yan, J., Xie, W., liu, C., and Qi, Z.: Influence of air pollution control devices on the polycyclic
           aromatic hydrocarbon distribution in flue gas from an ultralow-emission coal-fired power plant, Energy & Fuels, 30,
           9572-9579, http://doi.org/10.1021/acs.energyfuels.6b01381, 2016.

530   Li, J., Chen, H., Li, Z., Wang, P., Fan, X., He, W., and Zhang, J.: Analysis of low-level temperature inversions and their effects on aerosols in the lower atmosphere, Adv. Atmos. Sci., 36, 1235-1250, https://doi.org/10.1007/s00376-019-9018-9, 2019.

Lin, Y., Ma, Y., Qiu, X., Li, R., Fang, Y., Wang, J., Zhu, Y., and Hu, D. J. J. o. G. R. A.: Sources, transformation, and health implications of PAHs and their nitrated, hydroxylated, and oxygenated derivatives in PM2. 5 in Beijing, J. Geophys. Res., 120, 7219-7228, https://doi.org/10.1002/2015JD023628, 2015a.

535   Lin, Y., Qiu, X., Ma, Y., Ma, J., Zheng, M., and Shao, M.: Concentrations and spatial distribution of polycyclic aromatic hydrocarbons (PAHs) and nitrated PAHs (NPAHs) in the atmosphere of North China, and the transformation from PAHs to NPAHs, Environ. Pollut., 196, 164-170, https://doi.org/10.1016/j.envpol.2014.10.005, 2015b.

Lundgjerdingen, K. S.: Teknisk rapport Longyearbyen Energiverket (in Norwegian), Applica Test & Certification AS, Longyearbyen, Norway, Available by request from Longyearbyen Lokalstyre, 23, 2017.

540   Macdonal, R. W., Barrie, L. A., Bidleman, T. F., Diamond, M. L., Gregor, D. J., Semkin, R. G., Strachan, W. M., Li, Y. F., Wania, F., Alaee, M., Alexeeva, L. B., Backus, S. M., Bailey, R., Bewers, J. M., Gobeil, C., Halsall, C. J., Harner, T., Hoff, J. T., Jantunen, L. M., Lockhart, W. L., Mackay, D., Muir, D. C., Pudykiewicz, J., Reimer, K. J., Smith, J. N., and Stern, G. A.: Contaminants in the Canadian Arctic: 5 years of progress in understanding sources, occurrence and pathways, Sci. Total Environ., 254, 93-234, https://doi.org/10.1016/s0048-9697(00)00434-4, 2000.

545   Macdonald, C., Lockhart, L., and Gilman, A.: Effects of oil and gas activity on the environment and human health, in: Assessment 2007: Oil and gas activities in the Arctic - effect and potential effects, Arctic Monitoring and Assessment Programme (AMAP), Oslo, Norway, 5_1-5_164, 2010.

Marshall, C., Uguna, J., Large, D. J., Meredith, W., Jochmann, M., Friis, B., Vane, C., Spiro, B. F., Snape, C. E., and Orheim, A.: Geochemistry and petrology of palaeocene coals from Spitzbergen — Part 2: Maturity variations and

550   implications for local and regional burial models, Int. J. Coal Geol., 143, 1-10, https://doi.org/10.1016/j.coal.2015.03.013, 2015.

NILU: Observation data of atmospheric PAHs at Zeppelin and Birkenes stations, Norwegian Institute for Air Research, http://ebas.nilu.no, 2019

Noda, N., and Makino, H.: Influence of operating temperature on performance of electrostatic precipitator for pulverized

555   coal combustion boiler, Adv. Powder Technol., 21, 495-499, https://doi.org/10.1016/j.apt.2010.04.012, 2010.

Onduka, T., Ojima, D., Kakuno, A., Ito, K., Koyama, J., and Fujii, K.: Nitrated polycyclic aromatic hydrocarbons in the marine environment: acute toxicities for organisms at three trophic levels, Jpn. J. Environ. Toxicol., 15, 1-10, https://doi.org/10.11403/jset.15.1, 2012.

Pandey, P. K., Patel, K. S., and Lenicek, J.: Polycyclic aromatic hydrocarbons: need for assessment of health risks in India?

560   Study of an urban-industrial location in India, Environ. Monit. Assess., 59, 287-319, https://doi.org/10.1023/A:1006169605672, 1999.

Pedersen, H., Kallenborn, R., Ottesen, R., Gabrielsen, G., Schrum, C., Evenset, A., Ruus, A., Benjaminsen, H., Sagerup, K., and Christensen, G.: PCBs on Svalbard, Norwegian Environment Agency and Governor of Svalbard, Longyearbyen, Norway, 99 pp., 2011.

565   Peng, N., Li, Y., Liu, Z., Liu, T., and Gai, C.: Emission, distribution and toxicity of polycyclic aromatic hydrocarbons (PAHs) during municipal solid waste (MSW) and coal co-combustion, Sci. Total Environ., 565, 1201-1207, https://doi.org/10.1016/j.scitotenv.2016.05.188, 2016.

Ravindra, K., Wauters, E., and Van Grieken, R.: Variation in particulate PAHs levels and their relation with the transboundary movement of the air masses, Sci. Total Environ., 396, 100-110,

570   https://doi.org/10.1016/j.scitotenv.2008.02.018, 2008.

Reynaud, S., and Deschaux, P.: The effects of polycyclic aromatic hydrocarbons on the immune system of fish: A review, Aquat. Toxicol., 77, 229-238, http://10.1016/j.aquatox.2005.10.018, 2006.

Rogge, W. F., Hildemann, L. M., Mazurek, M. A., Cass, G. R., and Simoneit, B. R.: Sources of fine organic aerosol. 2. Noncatalyst and catalyst-equipped automobiles and heavy-duty diesel trucks, Environ. Sci. Technol., 27, 636-651,

575   https://doi.org/10.1021/es00041a007, 1993.

Schmale, J., Arnold, S. R., Law, K. S., Thorp, T., Anenberg, S., Simpson, W. R., Mao, J., and Pratt, K. A.: Local Arctic air pollution: A neglected but serious problem, Earth's Future, 6, 1385-1412, https://doi.org/10.1029/2018ef000952, 2018.

Shahpoury, P., Kitanovski, Z., Lammel, G. J. A. C., and Physics: Snow scavenging and phase partitioning of nitrated and

580   oxygenated aromatic hydrocarbons in polluted and remote environments in central Europe and the European Arctic, Atmos. Chem. Phys., 18, 13495-13510, https://doi.org/10.5194/acp-18-13495-2018, 2018.

Singh, D. K., Kawamura, K., Yanase, A., and Barrie, L. A.: Distributions of polycyclic aromatic hydrocarbons, aromatic ketones, carboxylic acids, and trace metals in Arctic aerosols: Long-range atmospheric transport, photochemical degradation/production at polar sunrise, Environ. Sci. Technol., 51, 8992-9004,

585   https://doi.org/10.1021/acs.est.7b01644, 2017.

Škrdlíková, L., Landlová, L., Klánová, J., and Lammel, G.: Wet deposition and scavenging efficiency of gaseous and particulate phase polycyclic aromatic compounds at a central European suburban site, Atmos. Environ., 45, 4305-4312, https://doi.org/10.1016/j.atmosenv.2011.04.072, 2011.

Tobiszewski, M., and Namieśnik, J.: PAH diagnostic ratios for the identification of pollution emission sources, Environ.

590   Pollut., 162, 110-119, https://doi.org/10.1016/j.envpol.2011.10.025, 2012.

UNECE: The 1998 Aarhus protocol on persistent organic pollutants (POPs), https://www.unece.org/env/lrtap/pops_h1.html, 49, 1998.

Wang, G., Ma, Z., Deng, J., Li, Z., Duan, L., Zhang, Q., Hao, J., and Jiang, J.: Characteristics of particulate matter from four coal–fired power plants with low–low temperature electrostatic precipitator in China, Sci. Total Environ., 662, 455-461, https://doi.org/10.1016/j.scitotenv.2019.01.080, 2019.

Wang, K., Shen, Y., Zhang, S., Ye, Y., Shen, Q., Hu, J., and Wang, X.: Application of spatial analysis and multivariate analysis techniques in distribution and source study of polycyclic aromatic hydrocarbons in the topsoil of Beijing, China, Environ. Geol., 56, 1041-1050, https://doi.org/10.1007/s00254-008-1204-5, 2009.

Wang, R., Liu, G., and Zhang, J.: Variations of emission characterization of PAHs emitted from different utility boilers of coal-fired power plants and risk assessment related to atmospheric PAHs, Sci. Total Environ., 538, 180-190, http://doi.org/10.1016/j.scitotenv.2015.08.043, 2015.

Wania, F., Mackay, D., and Hoff, J. T.: The importance of snow scavenging of polychlorinated biphenyl and polycyclic aromatic hydrocarbon vapors, Environ. Sci. Technol., 33, 195-197, https://doi.org/10.1021/es980806n, 1999.

Weinbruch, S., Benker, N., Kandler, K., Schutze, K., Kling, K., Berlinger, B., Thomassen, Y., Drotikova, T., and Kallenborn, R.: Source identification of individual soot agglomerates in Arctic air by transmission electron microscopy, Atmos. Environ., 172, 47-54, https://doi.org/10.1016/j.atmosenv.2017.10.033, 2018.

Willis, M. D., Leaitch, W. R., and Abbatt, J. P. D.: Processes controlling the composition and abundance of Arctic aerosol, Rev. Geophys., https://doi.org/10.1029/2018rg000602, 2018.

Wu, D., Wang, Z., Chen, J., Kong, S., Fu, X., Deng, H., Shao, G., and Wu, G.: Polycyclic aromatic hydrocarbons (PAHs) in atmospheric PM2.5 and PM10 at a coal-based industrial city: Implication for PAH control at industrial agglomeration regions, China, Atmos. Res., 149, 217-229, https://doi.org/10.1016/j.atmosres.2014.06.012, 2014.

Yang, H.-H., Lee, W.-J., Chen, S.-J., and Lai, S.-O.: PAH emission from various industrial stacks, J. Hazard. Mater., 60, 159-174, https://doi.org/10.1016/s0304-3894(98)00089-2, 1998.

Yu, Y., Katsoyiannis, A., Bohlin-Nizzetto, P., Brorström-Lundén, E., Ma, J., Zhao, Y., Wu, Z., Tych, W., Mindham, D., Sverko, E., Barresi, E., Dryfhout-Clark, H., Fellin, P., and Hung, H.: Polycyclic aromatic hydrocarbons not declining in Arctic air despite global emission reduction, Environ. Sci. Technol., 53, 2375-2382, https://doi.org/10.1021/acs.est.8b05353, 2019.

Yunker, M. B., Macdonald, R. W., Vingarzan, R., Mitchell, R. H., Goyette, D., and Sylvestre, S.: PAHs in the Fraser River basin: a critical appraisal of PAH ratios as indicators of PAH source and composition, Org. Geochem., 33, 489-515, https://doi.org/10.1016/s0146-6380(02)00002-5, 2002.

Zhang, L., Cheng, I., Muir, D., and Charland, J. P.: Scavenging ratios of polycyclic aromatic compounds in rain and snow in the Athabasca oil sands region, Atmos. Chem. Phys., 15, 1421-1434, https://doi.org/10.5194/acp-15-1421-2015, 2015.

Zhao, J., Zhang, J., Sun, L., Liu, Y., Lin, Y., Li, Y., Wang, T., and Mao, H.: Characterization of PM 2.5 -bound nitrated and oxygenated polycyclic aromatic hydrocarbons in ambient air of Langfang during periods with and without traffic restriction, Atmos. Res., 213, 302-308, https://doi.org/10.1016/j.atmosres.2018.06.015, 2018.

Zhao, S., Duan, Y., Yao, T., Liu, M., Lu, J., Tan, H., Wang, X., and Wu, L.: Study on the mercury emission and transformation in an ultra-low emission coal-fired power plant, Fuel, 199, 653-661, https://doi.org/10.1016/j.fuel.2017.03.038, 2017.

Zheng, L., Ou, J., Liu, M., Chen, Y., Tang, Q., and Hu, Y.: Seasonal and spatial variations of PM10-bounded PAHs in a coal mining city, China: Distributions, sources, and health risks, Ecotox. Environ. Safe., 169, 470-478, https://doi.org/10.1016/j.ecoenv.2018.11.063, 2019.

Zielinska, B., Arey, J., Atkinson, R., and McElroy, P. A.: Formation of methylnitronaphthalenes from the gas-phase reactions of 1-and 2-methylnaphthalene with hydroxyl radicals and nitrogen oxide (N2O5) and their occurrence in ambient air, Environ. Sci. Technol., 23, 723-729, https://doi.org/10.1021/es00064a011, 1989.

Zielinska, B., Sagebiel, J., McDonald, J. D., Whitney, K., and Lawson, D. R.: Emission rates and comparative chemical composition from selected in-use diesel and gasoline-fueled vehicles, J Air Waste Manag Assoc, 54, 1138-1150, https://doi.org/10.1080/10473289.2004.10470973, 2004.

640   **Table 1.** Concentrations of PAHs (G+P) and percentage in the particulate phase (%PM) in Longyearbyen power plant, UNIS, and Adventdalen. Data are average, minimum and maximum, n=6 for each location[*].

Compound name	Abbreviated name	Power plant			UNIS			Adventdalen		
		Mean ng m⁻³	Min-Max ng m⁻³	Mean %PM	Mean pg m⁻³	Min-Max pg m⁻³	Mean %PM	Mean pg m⁻³	Min-Max pg m⁻³	Mean %PM
Naphthalene	Nap	51.82	32.74-59.82	7.4	<MDL	<MDL	-	<MDL	<MDL	-
Acenaphtylene	Acy	2.30	1.22-3.80	0.6	16.89	7.14-29.15	0.0	2.40	1.10-5.13	0.0
Acenaphthene	Ace	0.87	0.30-2.18	8.4	48.48	24.29-72.99	0.0	3.84	1.25-6.62	0.0
Fluorene	Flu	7.61	3.68-12.16	4.6	170.50	136.5-236.0	1.1	59.96	38.49-95.82	1.8
Phenanthrene	Phe	27.32	12.01-44.87	5.6	409.20	368.5-470.0	6.5	236.30	191.7-270.8	3.7
Anthracene	Ant	1.06	0.23-2.13	0.0	18.04	12.29-25.52	0.0	14.25	10.46-19.33	3.5
Fluoranthnene	Flt	6.99	1.43-12.49	3.9	28.45	24.14-36.06	40.5	19.14	10.76-38.54	23.2
Pyrene	Pyr	4.40	1.08-7.35	8.3	39.47	30.72-47.84	26.8	27.17	20.91-35.89	15.8
Benzo(a)anthracene	BaAnt	0.13	0.04-0.20	0.0	2.17	0.01-5.83	68.2	n.d.	n.d.	-
Chrysene	Chry	0.28	0.06-0.42	0.0	7.32	2.60-13.47	81.7	3.12	0.11-7.11	64.1
Benzo(b+k)fluoranthene	BbkFlt	n.d.	n.d.	-	2.23	0.01-5.87	100.0	0.75	0.01-2.79	100.0
Benzo(a)pyrene	BaPyr	n.d.	n.d.	-	0.89	0.01-2.46	100.0	0.34	0.01-1.16	100.0
Indeno(1.2.3-cd)pyrene	IPyr	n.d.	n.d.	-	1.63	0.07-3.79	100.0	0.71	0.07-2.67	100.0
Dibenzo(a.h)anthracene	DBAnt	n.d.	n.d.	-	n.d.	n.d.	-	n.d.	n.d.	-
Benzo(g.h.i)perylene	BPer	n.d.	n.d.	-	3.92	1.44-8.12	100.0	1.21	0.08-3.83	100.0
∑16 PAHs		102.8	61.9-139.1	-	749.2	687.4-866.9	-	369.1	279.0-454.5	-
9-Fluorenone	9-Flu	12.35	5.57-19.54	19.2	270.30	128.2-543.8	41.7	139.40	110.2-177.2	25.5
9,10-Anthraquinone	9,10-AntQ	15.76	4.60-47.00	21.3	163.50	105.2-269.1	37.5	71.70	11.4-118.4	43.9
4H-Cyclopenta(def)-phenanthrene-4-one	cPPhe-4	1.30	0.51-2.55	15.8	27.23	20.16-35.80	65.5	18.77	11.97-39.10	38.1
9,10-Phenanthrenequinone	9,10-PheQ	2.13	0.96-4.40	0.0	<MDL	<MDL	-	<MDL	<MDL	-
Benzo(a)fluoren-11-one	BaFlu-11	0.16	0.08-0.23	27.6	6.07	1.79-11.08	100.0	2.23	0.71-4.36	100.0
Benzanthrone	BZT	0.87	0.14-1.31	0.0	1.76	0.02-4.32	96.7	0.10	0.02-0.58	100.0
Benzo(a)anthracene-7,12-dione	BaAnt-7,12	n.d.	n.d.	-	2.20	0.01-4.86	100.0	0.93	0.01-2.21	100.0
6H-Benzo(cd)pyren-6-one	BPyr-6	n.d.	n.d.	-	n.d.	n.d.	-	n.d.	n.d.	-
∑8 OPAHs		32.6	15.8-73.1	-	471.0	325.9-741.4	-	233.1	124.7-337.1	-
1-Nitronaphthalene	1-NNap	2.19	0.99-4.69	61.7	16.97	13.36-21.53	0.1	5.02	1.91-9.84	1.5
2-Nitronaphthalene	2-NNap	0.26	0.11-0.40	31.7	5.08	2.44-7.33	3.1	1.88	1.29-2.83	5.4
2-Nitrobiphenyl	2-NBip	0.16	0.07-0.29	39.9	0.99	0.82-1.20	10.1	0.98	0.81-1.29	5.9
4-Nitrobiphenyl	4-NBip	n.d.	n.d.	-	2.23	1.51-2.68	0.0	2.45	0.29-4.10	0.0
1,5-Dinitronaphthalene	1,5-DNNap	n.d.	n.d.	-	0.80	0.05-2.17	80.0	0.93	0.05-3.72	53.9
5-Nitroacenaphthene	5-NAce	n.d.	n.d.	-	0.15	0.05-0.38	0.0	0.30	0.05-1.62	0.0
2-Nitrofluorene	2-NFlu	0.04	0.02-0.14	0.0	0.21	0.07-0.78	15.1	0.59	0.07-1.05	4.2
9-Nitroanthracene	9-NAnt	0.08	0.02-0.23	0.0	0.62	0.19-0.91	n.d.	2.26	0.12-4.70	57.8
9-Nitrophenanthrene	9-NPhe	n.d.	n.d.	-	0.20	0.09-0.37	n.d.	0.44	0.09-1.17	25.0
3-Nitrophenanthrene	3-NPhe	0.76	0.0003-1.93	96.1	n.d.	n.d.	-	n.d.	n.d.	-
2-Nitroanthracene	2-NAnt	0.31	0.07-0.62	0.0	n.d.	n.d.	-	n.d.	n.d.	-
2+3-Nitrofluoranthene	2+3-NFlt	0.52	0.06-1.14	0.0	9.50	7.32-11.37	94.5	12.30	4.68-26.66	79.8
4-Nitropyrene	4-NPyr	0.11	0.03-0.17	0.0	n.d.	n.d.	-	n.d.	n.d.	-
1-Nitropyrene	1-NPyr	n.d.	n.d.	-	n.d.	n.d.	-	n.d.	n.d.	-
2.7-Dinitrofluorene	2,7-DNFlu	0.06	0.001-0.14	0.0	n.d.	n.d.	-	n.d.	n.d.	-
7-Nitrobenzo(a)anthracene	7-NBaAnt	0.58	0.11-0.93	0.0	n.d.	n.d.	-	n.d.	n.d.	-
6-Nitrochrysene	6-NChry	n.d.	n.d.	-	n.d.	n.d.	-	n.d.	n.d.	-
1,3-Dinitropyrene	1,3-DNPyr	n.d.	n.d.	-	n.d.	n.d.	-	n.d.	n.d.	-
1,6-Dinitropyrene	1,6-DNPyr	n.d.	n.d.	-	n.d.	n.d.	-	n.d.	n.d.	-

1,8-Dinitropyrene	1.8-DNPyr	n.d.	n.d.	-	n.d.	n.d.	-	n.d.	n.d.	-
6-Nitrobenzo(a)pyrene	6-NBaPyr	n.d.	n.d.	-	n.d.	n.d.	-	n.d.	n.d.	-
∑22 NPAHs		4.5	2.0-7.8	-	36.8	30.3-46.1	-	27.2	13.5-44.4	-

*Full results are given in SI (Table S9-S11)

<MDL below method detection limit

645   n.d. not detected

Table 2. Ratios of individual oxy- and nitro-PAHs to their corresponding parent PAHs in Longyearbyen power plant (G+P; n=6).

Ratio	Mean	STD
Nitro-PAH/PAH		
2-NFlu/Flu	0.004	0.005
3-NPhe/Phe	0.028	0.028
2-NAnt/Ant	0.150	0.107
9-NAnt/Ant	0.040	0.028
2+3-NFlt/Flt	0.030	0.023
7-NBaAnt/BaAnt	5.37	3.87
Oxy-PAH/PAH		
9,10-PheQ/Phe	0.08	0.01
cPPhen-4/Pyr	0.31	0.10
BaFlu-11/Chry	0.65	0.34
9-Flu/Phe	0.47	0.13
9-Flu/Flu	1.67	0.29
9,10-AntQ/Ant	12.17	7.30

650

Table 3. PAHs diagnostic ratios for the Longyearbyen power plant (G+P; n=6).

Ratio	Mean	STD
Ant/(Ant+Phe)	0.044	0.002
Flt/(Flt+Pyr)	0.606	0.025
Flu/(Flu+Pyr)	0.638	0.110
BaAnt/(BaAnt+Chry)	0.332	0.027

655 **Table 4.** Source identification based on diagnostic ratios derived from total (G+P) concentrations; average of individual ratio values (n=6) with standard deviation are presented

	Ratio	Potential sources	Reference
IPyr/(IPyr+BPer)			
Power plant	n.d.	-	
UNIS	0.32±0.01	<0.35 Gasoline	(Ravindra et al., 2008)
Adventdalen	0.45±0.05	0.35-0.70 Diesel	(Kavouras et al., 2001), (Ravindra et al., 2008)
Flu/(Flu+Pyr)			
Power plant	0.64±0.11	-	
UNIS	0.81±0.04	>0.5 coal combustion	(Yunker et al., 2002), (Katsoyiannis and Breivik, 2014)
		>0.5 Diesel	(Ravindra et al., 2008)
Adventdalen	0.68±0.05	0.64 local power plant	This study (Table 3)
		>0.5 coal combustion	(Yunker et al., 2002), (Katsoyiannis and Breivik, 2014)
BaPyr/(BaPyr +Chry)			
Power plant	n.d.	-	
UNIS	0.12±0.07	<0.2 Petrogenic source	(Wu et al., 2014)
Adventdalen	0.16±0.04	<0.2 Petrogenic source	(Wu et al., 2014)
BaPyr/BPer			
Power plant	n.d.	-	
UNIS	0.34±0.14	<0.6 Vehicular emissions	(Pandey et al., 1999)
Adventdalen	0.45±0.20	<0.6 Vehicular emissions	(Pandey et al., 1999)
BaAnt/(BaAnt+ Chry)			
Power plant	0.33±0.03	-	
UNIS	0.30±0.04	0.33 coal combustion	This study (Table 3)
		0.2-0.35 coal combustion	(Akyüz and Çabuk, 2010)
Adventdalen	n.d.	-	
IcdP/BghiP			
Power plant	n.d.	-	
UNIS	0.39±0.20	<0.4 Gasoline	(Ravindra et al., 2008)
Adventdalen	0.81±0.16	~1 Diesel	(Ravindra et al., 2008)
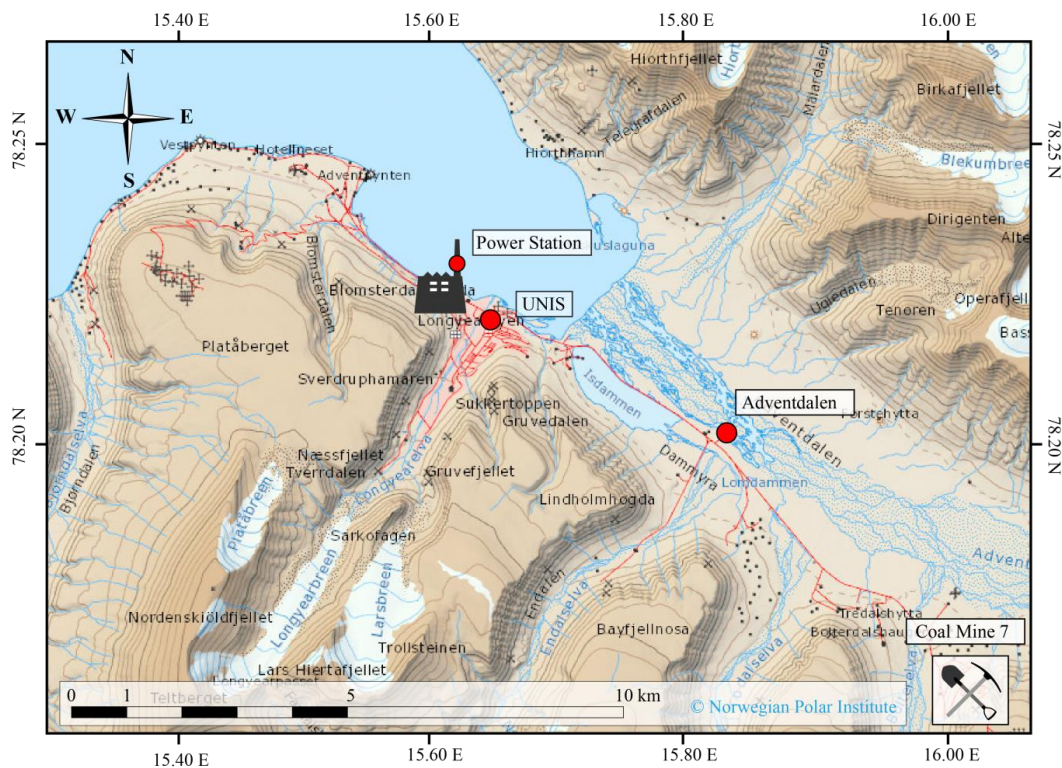
Figure 1. Air sampling transect locations in the vicinity of Longyearbyen.

660
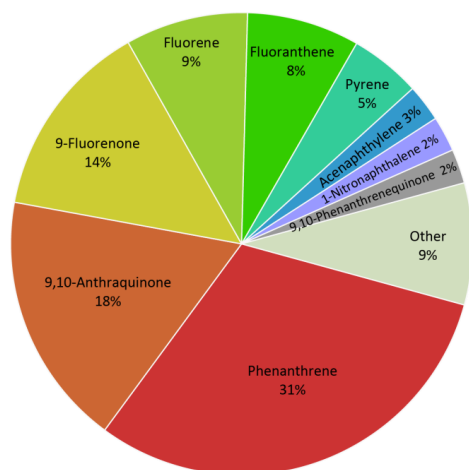
Figure 2. Proportion of PAH derivatives (G+P; excluding Nap) in the Longyearbyen power plant emission (n=6).

665
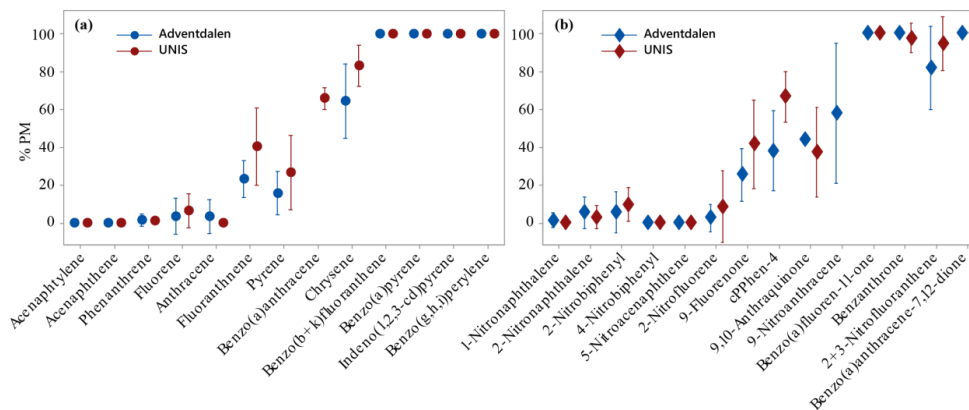
Figure 3. Percentage of (a) PAHs and (b) nitro- and oxy-PAHs determined in particulate phase (% PM) at UNIS (n=6) and Adventdalen (n=6); individual standard deviations are used to calculate the intervals.

670
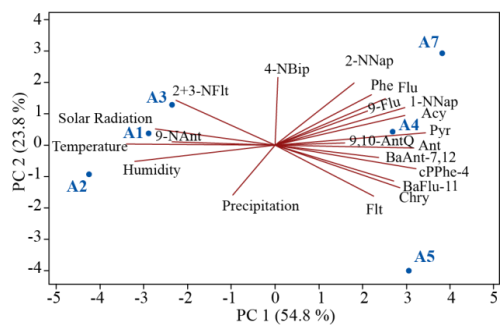
Figure 4. Principal component analysis biplot of PC1 and PC2 for Adventdalen samples (G+P; n=6).

675
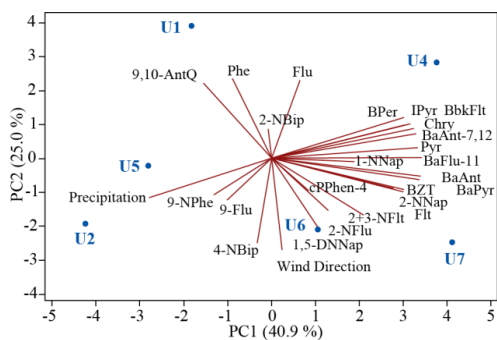
Figure 5. Principal component analysis biplot of PC1 and PC2 for UNIS samples (G+P; n=6).

680
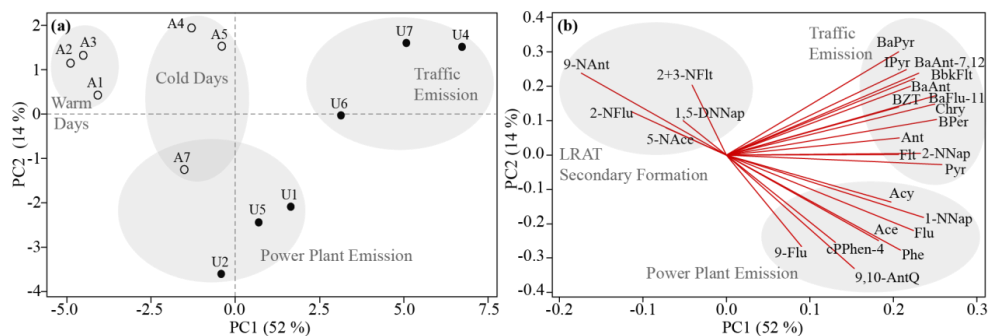
Figure 6. Score (a) and loading (b) plots of PC1 and PC2 for Adventdalen (A) and UNIS (U) samples together (G+P; n=12).